Pore Collapse during the Fabrication Process of Rubber-Like Polymer Scaffolds

Raúl Brígido Diego,[1] José Luis Gómez Ribelles,[1,2] Manuel Salmerón Sánchez[1,2]

[1]*Center for Biomaterials, Universidad Politécnica de Valencia, 46022 Valencia, Spain*
[2]*Centro de Investigación Príncipe Felipe, Autopista del Saler 16, 46013 Valencia, Spain*

Received 6 April 2006; accepted 26 July 2006
DOI 10.1002/app.25202
Published online in Wiley InterScience (www.interscience.wiley.com).

ABSTRACT: Rubbery polymer scaffolds for tissue engineering were produced using templates of the pore structure. The last step in the fabrication process consists of dissolving the template using a solvent that, at the same time, swells the scaffolding matrix that was a polymer network. Sometimes the polymer matrix is stretched so strongly that when the solvent is eliminated, i.e., the network is dried, it shrinks and is not able to recover its original shape and, consequently, the porous structure collapses. In this work we prepared, using the same fabrication process (the same template and the same solvent), a series of polymer scaffolds that results in collapsed or noncollapsed porous structures, depending on the polymer network composition. We explain the collapse process as a consequence of the huge volume increase in the swelling process during the template extraction due to the large distance between crosslinking points in the scaffolding matrix. By systematically increasing the crosslinking density the porous structure remains after network drying and the final interconnected pores were observed. It is shown that this problem does not take place when the scaffolding matrix consists of a glassy polymer network. © 2007 Wiley Periodicals, Inc. J Appl Polym Sci 104: 1475–1481, 2007

Key words: scaffolds; collapsed structure; hydrophobic; tissue engineering

INTRODUCTION

Polymer scaffolds play an important role in the regeneration of damaged tissues and organs as supporting structures for cell attachment, proliferation, and guidance of new tissue formation, i.e., they constitute a synthetic extracellular matrix. Scaffolds should be designed so as to show adequate properties that satisfy the specific biological, mechanical, and geometrical requirements.[1–4] These structures must be porous and permeable to permit the ingress of cells and nutrients and should exhibit the appropriate surface chemistry for cell attachment and proliferation.[5–7] It is important to prepare scaffolds with controlled architecture, total porosity, as well as pore size, since these factors are associated with supplying nutrients to transplanted and regenerated cells, and thus are critical factors in tissue regeneration.[3,8] Adequate pore size is normally in the range of 50μm to permit the ingrowth of cells, vascularization, and regeneration of the tissue.[9,10]

Several methods have been proposed for the preparation of polymer scaffolds such as phase separation,[3] emulsion freeze-drying,[11] gas foaming,[12] fiber templates,[13] porogen leaching,[14,15] and solid free fabrication (SFF)-rapid prototyping (RP), techniques that involve building 3D objects using layered manufacturing methods.[16] The method we employed in this work is based on the use of templates for generating the porous structure. It consists of forming a bonded microsphere template that it is dissolved (using the appropriate solvent) after the polymerization process, getting the scaffolding structure polymerized between the free space of the template. This technique allows controlling the interconnectivity between pores and their size without requiring special machines.[17,18] Nevertheless, under some circumstances it is found that the interconnected pore structure is collapsed after the final fabrication process, especially when the scaffolding matrix is in a rubber-like state. Even though this is a problem cited in the literature for several polymer structures,[19–21] this is, to our knowledge, the first time that the pore collapse of macroporous structures fabricated by means of templates was investigated systematically.

The objective of this work is to study the pore collapse in different rubber-like polymer scaffolds with interconnected spherical pores during the drying process after template extraction by means of a good solvent, both for the template and the scaffolding network. We have used hydrophobic acrylates with good response in cell culture.[22–24] We identify the swelling degree of the polymer network that constitutes the

Correspondence to: M. Salmerón Sánchez (masalsan@fis.upv.es).

Contract grant sponsor: Spanish Ministry of Science and Education; contract grant number: MAT2004-04980-C02-01.

scaffolds walls as the key factor to be controlled in order to achieve the desired noncollapsed structure.

EXPERIMENTAL

Materials

Commercial poly(methyl methacrylate) microspheres of different diameters: 35 ± 10 μm (PMMA, Colacryl TS1881), 90 ± 10 μm, (PMMA, Colacryl dp 300), and PMMA obtained by classical suspension polymerization with diameter 250 ± 10 μm or 550 ± 50 μm were used as porogen templates. Ethyl acrylate (EA), ethyl methacrylate (EMA), and buthyl acrylate (BA) (Aldrich, Milwaukee, WI, 99% pure) were used as monomers, benzoin (Scharlau, Barcelona, Spain, 98% pure) as photoinitiator. Two crosslinkers were employed: ethyleneglycol dimethacrylate (EGDMA) and triethyleneglycol dimethacrylate (TEGDMA) (Aldrich, 99% pure).

Preparation of the scaffolds

The preparation of the scaffolds was done as described elsewhere.[17,18] Briefly, PMMA microspheres were introduced between two plates (of a self-built device) whose distance can be controlled by adjusting the step of a coupled screw and heated at 180°C for 30 min to obtain the first template. To obtain scaffolds with controlled porosity, the thickness of the obtained disk was first measured, then the disk was replaced in the mold and compressed at 180°C for 30 min. After cooling the template at room temperature, a monomer solution was introduced in the empty space between the PMMA spheres. The solution consisted of the monomer (in this work we employed EA and mixtures of the comonomers EMA and BA), the molecular crosslinker (we used either TEGDMA or EGDMA), and 0.2 wt % of benzoin as a photoinitiator. The polymerization was carried out up to limiting conversion under UV radiation at room temperature. After polymerization took place the PMMA matrix was removed by soxhlet extraction with diclorometha ne for 48 h. At this stage the PMMA porogen template was completely removed. The porous sample was kept 24 h more in a soxhlet with ethanol in order to extract low molecular weight substances. Samples were dried in vacuo to constant weight before characterization.

Characterization of the scaffolds

The volume fraction of pores in the scaffold, the porosity, was determined gravimetrically by swelling the sample in water using a vacuum accessory. The porosity P is defined as:

$$P = \frac{V_{pore}}{V_{pore} + V_{polymer}}, \quad (1)$$

where V_{pore} is the part of the volume occupied by pores and $V_{polymer}$ is the volume occupied by the polymer. Let m_s^{sw} be the mass of the scaffold swollen in water and m_s^d the mass of the dry scaffold. Since the matrix material of the scaffold is hydrophobic, we neglect the small amount of water that is absorbed in immersion (∼ 0.7 wt %). The mass of water located in pores m_w^{pores} is:

$$m_w^{pores} = m_s^{sw} - m_s^d. \quad (2)$$

Taking into account the density of water, ρ_w, the amount of water located in pores gives their volume:

$$V_{pore} = \frac{m_s^{sw} - m_s^d}{\rho_w}. \quad (3)$$

On the other hand, the volume of the scaffold occupied by the polymer can be obtained by measuring the density of the corresponding bulk material, ρ_b:

$$V_{polymer} = \frac{m_s^d}{\rho_b}. \quad (4)$$

ρ_b was determined by weighting each of the samples both in air and immersed in *n*-octane at 25°C (Table I). A Mettler (Columbus, OH) AE240 balance (sensitivity 0.01 mg) with density accessory Mettler ME3360 was employed. Porosity measurements were done in at least three samples of each of the compositions; porosity values were reproducible up to 3%.

Scanning electron micrography (SEM) was performed with a Hitachi (Tokyo, Japan) S-3200N device. Transversal and longitudinal slices of the dry samples were coated with gold before observation at 15 kV.

Dynamic mechanical spectroscopy was performed with a Seiko (Tokyo, Japan) DMS 210 apparatus at a frequency of 1 Hz in the tension mode. The temperature dependence of the storage modulus E′ and the loss angle were measured in a temperature range from −150 to 180°C at a rate of 2°C/min. The samples for these experiments were prismatic (∼10 × 4.5 × 0.9 mm^3).

TABLE I
Bulk Density and Glass Transition Temperature of the Different Networks

Polymer network	Bulk density (g/cm^3)	T_g (°C)
EA/EGDMA (98/2)	1.130	−12.0
EA/TEGDMA (98/2)	1.126	−14.4
EA/TEGDMA (95/5)	1.132	−12.9
EA/TEGDMA (90/10)	1.140	−11.1
EA/TEGDMA (80/20)	1.154	−5.1
EA/TEGDMA (70/30)	1.160	4.3
(EMA/BA)/EGDMA ((79/19)/2)	1.125	48.5

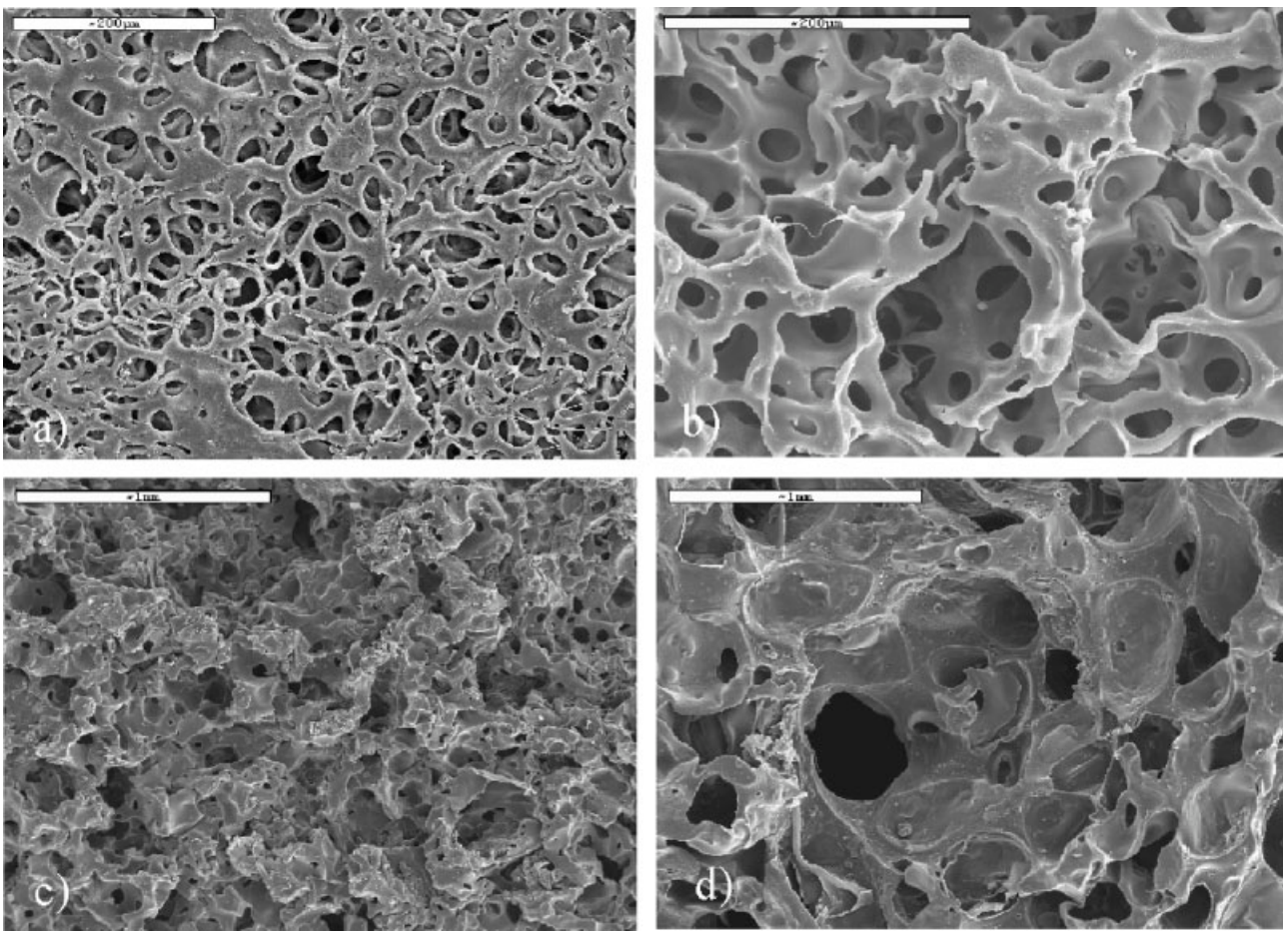

Figure 1 SEM micrographs of the collapsed structure obtained in the fabrication process of PEA/EGDMA (98/2) scaffolds. The same total porosity (75%) and four different pore sizes: (a) 35 μm, (b) 90 μm, (c) 250 μm, and (d) 500–600 μm.

The sorption of dichloromethane by the bulk samples in immersion was determined by soaking the dry samples in the solvent for 3 days at 25°C and measurement of their weight after gentle drying of the surface.

RESULTS AND DISCUSSION

Figure 1 shows the SEM micrographs of several collapsed structures obtained after removing the PMMA template with dichloromethane (the theoretical porosity attained, i.e., the volume fraction of PMMA in the template, should have been ~ 70%). The matrix consists of a polymer network of polyethyl acrylate (PEA) crosslinked with 2 wt % EGDMA. The structure collapses for any pore size ranging from 35 μm. During the solution process of the PMMA template the scaffolding matrix network is stretched so strongly that when the dichloromethane is changed to ethanol the network shrinks and is not able to recover its initial shape (Table I shows the glass transition temperature for this network). The difference in the pore structure between the swollen and the dry states has shown in the literature[25,26] for systems with much smaller pores. In addition, the influence of the type of the solvent used has also been reported.[27–42] Polymer porous structures dried from bad solvents show maximum porosity that is close to the porosity in the swollen state.[35] The drying process of polymers swollen in good solvents may lead to a partial or total collapse of the pores.[39,40] These experimental findings indicate that the porosity attained in the swollen state can be preserved in the dry state if the interactions between the polymer and the solvent are decreased before the drying process. Conversely, since the swelling of a polymer network by a solvent depends also on the network parameters, i.e., the number of elastically active chains, we decided to increase the crosslinking degree of the network so as to reduce the swelling degree and, consequently, prevent the collapse of the structure after solving the template and drying the network.

According to the theory of rubber elasticity, the molar concentration of elastically active, or effective, chains n_c/V is related to the rubber modulus by:[43]

$$E' = \frac{n_c}{V_2} 3RT = \frac{d_2}{M_c} 3RT. \quad (5)$$

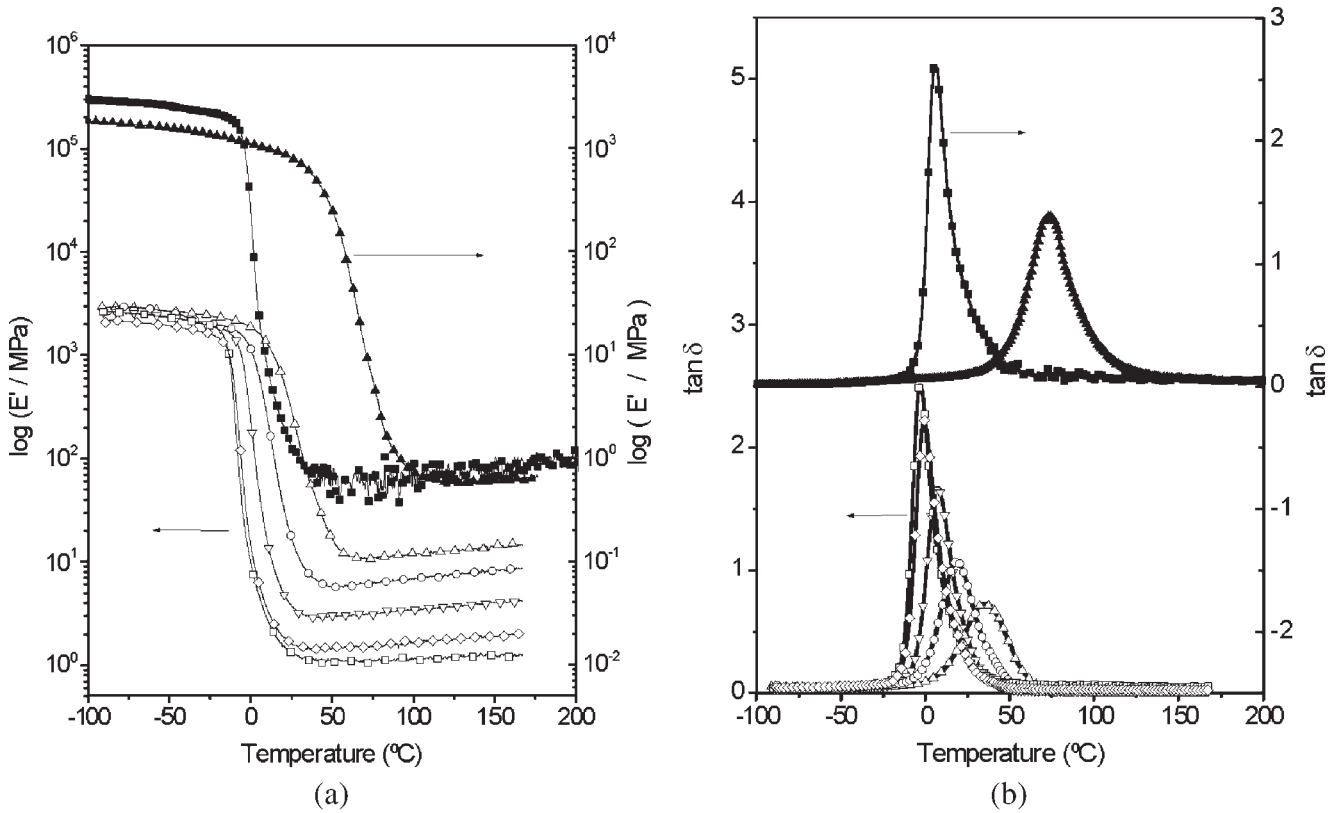

Figure 2 (a) Dynamic mechanical storage modulus. (b) Tangent of the dynamic mechanical loss angle versus the temperature at 1 Hz for the polymer networks. (□) PEA crosslinked with 2%TEGDMA, (◇) 5%TEGDMA, (▽) 10%TEGDMA, (○) 20%TEGDMA, (△) 30%TEGDMA, (■) PEA crosslinked with 2%EGDMA, (▲) P(EMA-*co*-BA) copolymer crosslinked with 2%EGDMA.

Where R is the universal gas constant, T is the absolute temperature, E' is the modulus in the elastomeric region at T, M_c is the molecular weight between crosslinks, and d_2 is the network density. We measured the densities of our networks at room temperature ($\sim$ 298 K), then M_c can be calculated with the experimental E' values in the rubbery region calculated from the dynamic mechanical measurements shown in Figure 2. The rubbery modulus increases as the crosslinking density does [Fig. 2(a)] and, at the same time, the main mechanical relaxation moves to higher temperatures [Fig. (2b)]. The data employed for the calculations are given in Table II. We used the molecular crosslinker TEGDMA (instead of EGDMA) because TEGDMA is a more flexible molecule than EGDMA and it allows higher crosslinking density without the presence of internal stresses in the polymer network that might lead to the formation of microcracks during the polymerization process. n_c/V_2 increases as the amount of TEGDMA in the system does and, consequently, the molecular weight M_c between crosslinks decreases (Table II).

The Flory-Rehner equation[43] relates the swelling degree to the polymer–solvent interaction and the

TABLE II
Properties of the Polymer Networks

Polymer network	E′ (MPa)	n_c/V_2 (mol/cm^3)	M_c (g/mol)	w	ϕ_1	$\overline{\chi}_{12}$
EA/EGDMA (98/2)	0.857	1.135E-10	9992.7	8.88	0.91	0.13
EA/TEGDMA (98/2)	1.074	1.423E-10	7914.5	6.97	0.89	0.27
EA/TEGDMA (95/5)	1.601	2.120E-10	5340.4	4.74	0.85	0.25
EA/TEGDMA (90/10)	3.342	4.426E-10	2575.6	2.90	0.77	0.26
EA/TEGDMA (80/20)	6.745	8.933E-10	1291.8	1.67	0.66	0.32
EA/TEGDMA (70/30)	11.527	1.527E-09	759.9	1.23	0.58	0.28
(EMA/BA)/EGDMA ((79/19)/2)	0.551	7.299E-11	5928.9	4.79	0.85	0.27

E′ = measured storage modulus at 100°C; n_c/V_2 = density of elastically active chains; M_c = molecular mass between crosslinks; w = dichloromethane sorption capacity of the materials (mass of solvent per unit mass of the dry network); ϕ_1 = equilibrium volume fraction of solvent in the network; $\overline{\chi}_{12}$ = apparent interaction parameter.

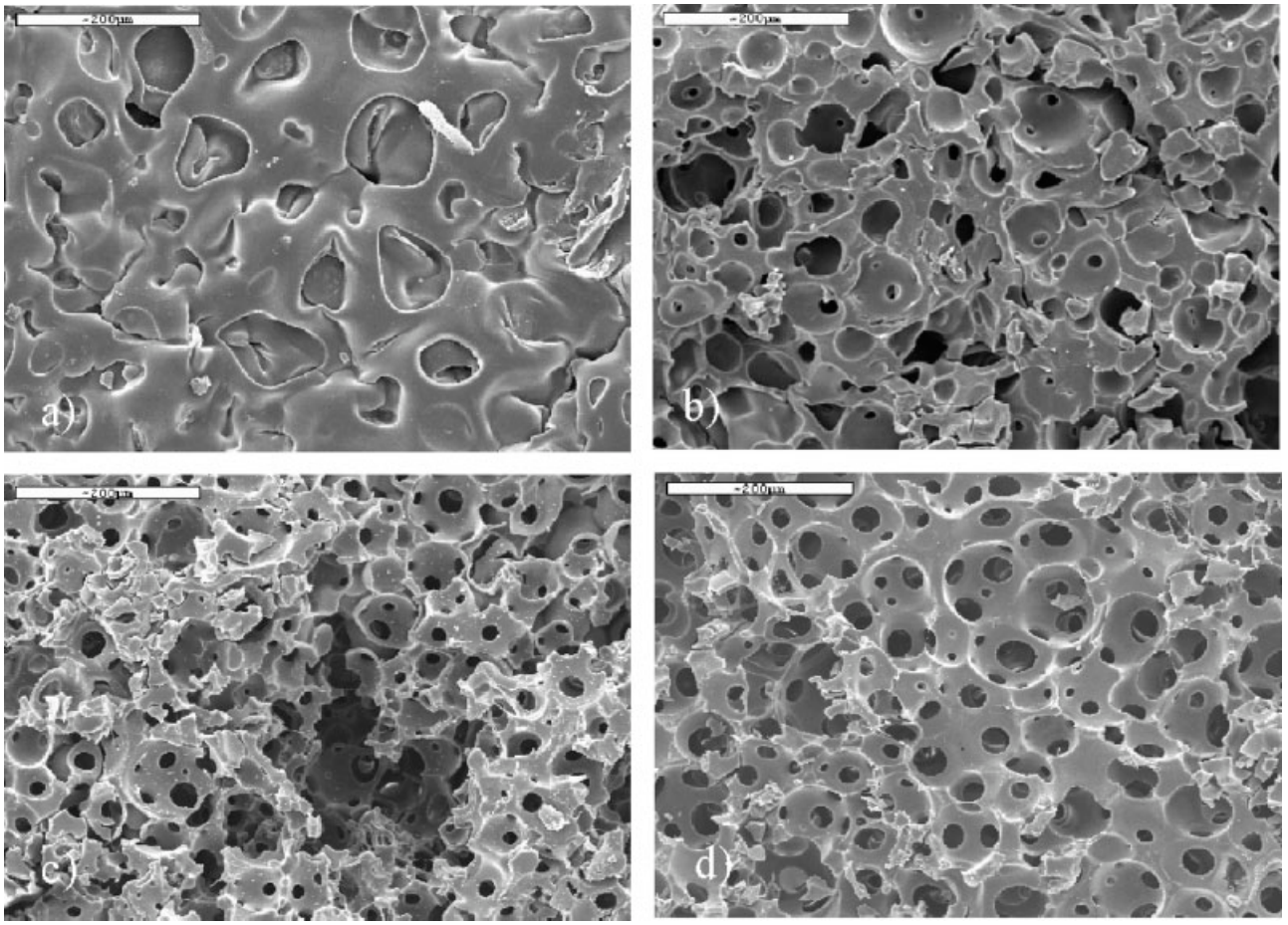

Figure 3 SEM micrographs of PEA scaffolds with varying crosslinking density, constant porosity 75%, and pore size (90 μm); (a) 2%TEGDMA, (b) 5%TEGDMA, (c) 20%TEGDMA, and (d) 30%TEGDMA.

topological parameters of the network:

$$0 = \ln \phi_1 + 1 - \phi_1 + \overline{\chi}_{12}(1 - \phi_1)^2 + \mathbf{v}_1 \frac{n_c}{V_2}(1 - \phi_1)^{\frac{1}{3}}. \tag{6}$$

In this equation, ϕ_1 is the equilibrium volume fraction of the solvent in the gel, $\mathbf{v}_1$ is the molar volume of the solvent (64.26 cm^3/mol for the dichloromethane), $\overline{\chi}_{12}$ is the apparent interaction parameter, and n_c/V_2 is the volume density of elastically active chains in the network. We decided to increase n_c/V by changing the crosslinker/monomer ratio during the polymerization process that leads to the network formation. ϕ_1 was calculated from the gravimetrically measurement of the quantity w, the ratio of the mass of dichloromethane absorbed to the mass of the dry polymer before immersion, and the polymer density d_2

$$\phi_1 = \frac{w}{w + \frac{d_1}{d_2}}. \tag{7}$$

ϕ_1 decreases as the crosslinking density increases, while $\overline{\chi}_{12}$, as calculated from Eq. 1, remains almost constant (Table II). The low value (below 0.5) of the interaction

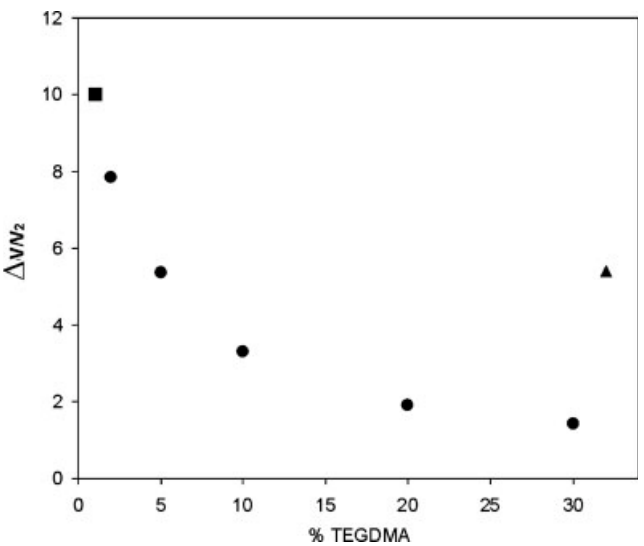

Figure 4 Volume increment as a consequence of the swelling process in dichloromethane process relative to the volume of the dry network V_2. The square represents the volume increment for the EA/EGDMA (98/2) polymer network and the triangle the volume increment for the (EMA/BA)/EGDMA copolymer network.

TABLE III
Thickness of the Polymer Scaffold before and after the Extraction of the PMMA Template

Polymer network	Initial thickness (mm)	Final thickness (mm)	Reduction (%)
EA/TEGDMA (98/2)	2.5	1.1	54
EA/TEGDMA (95/5)	2.7	1.3	52
EA/TEGDMA (90/10)	2.7	1.8	33
EA/TEGDMA (80/20)	2.6	2.1	19
EA/TEGDMA (70/30)	2.6	2.4	10

The thickness reduction quantifies the collapse of the structure.

parameter indicates that dichloromethane is a good solvent both for PEA and the crosslinker TEGDMA. The effect of increasing the TEGDMA content in the system does not influence the nature of the polymer–solvent interaction and, consequently, the steady decrease in the equilibrium solvent content can only be explained by the increase in the density of elastically active chains n_c/V_2 in the system; i.e., the decrease of the molecular weight M_c between crosslinks.

Figure 3 shows four micrographs of scaffolds prepared with the same pore size (90 μm) and the total theoretical porosity according to the fabrication process (~75%).[18] Pores are collapsed for low crosslinking density, but the open structure of the interconnected spherical pores is reached as the amount of TEGDMA increases. Figure 4 shows the volume increase in the swollen network relative to the volume of the dry one as calculated from Table II:

$$\frac{\Delta V}{V_2} = \frac{d_2}{d_1} w. \tag{8}$$

Higher crosslinking densities reduce the volume augmentation during the swelling process, which prevents the collapse of the scaffolding structure after removing the PMMA template. The pore collapse can be quantified by measuring the sample thickness before and after the PMMA template extraction. Table III shows the corresponding thickness reduction. Up to 10 wt % TEGDMA the pore collapse is almost complete. The thickness reduction decreases up to ~ 10 % for TEGDMA contents higher than 30 wt %, in which the interconnected open structure is nicely depicted in Figure 3(d). Then the composition 70/30 EA/TEGDMA allows one to keep the interconnected open structure after eliminating the PMMA template and drying the network. Several polymer scaffolds have been fabricated successfully by using this composition with different pore sizes and in a broad porosity range.[18]

The pore collapse is not such a critical problem when the scaffolding matrix is in the glassy state after the drying process. We fabricated similar interconnected spherical structures by using a copolymer of EA/BA 80/20 wt % with 1 wt % EGDMA. The glass transition temperature as measured by DSC is ~ 48°C (Table I). The resulting scaffold of total porosity (~ 75%) shows interconnected spherical pores of 90 μm (Fig. 5). The equilibrium volume fraction of solvent in the network is 0.85. Such a high solvent content is reached because of the good polymer–solvent interaction parameter ($\overline{\chi}_{12} = 0.27$) and low density of elastically active chains ($n_c/V_2 = 7.299 \times 10^{-11}$ mol/cm^3) (see Table II). This network increases its volume almost six times (see Fig. 2) during the PMMA template extraction due to the swelling process. However, as the copolymer is dried the glass transition temperature increases above room temperature and

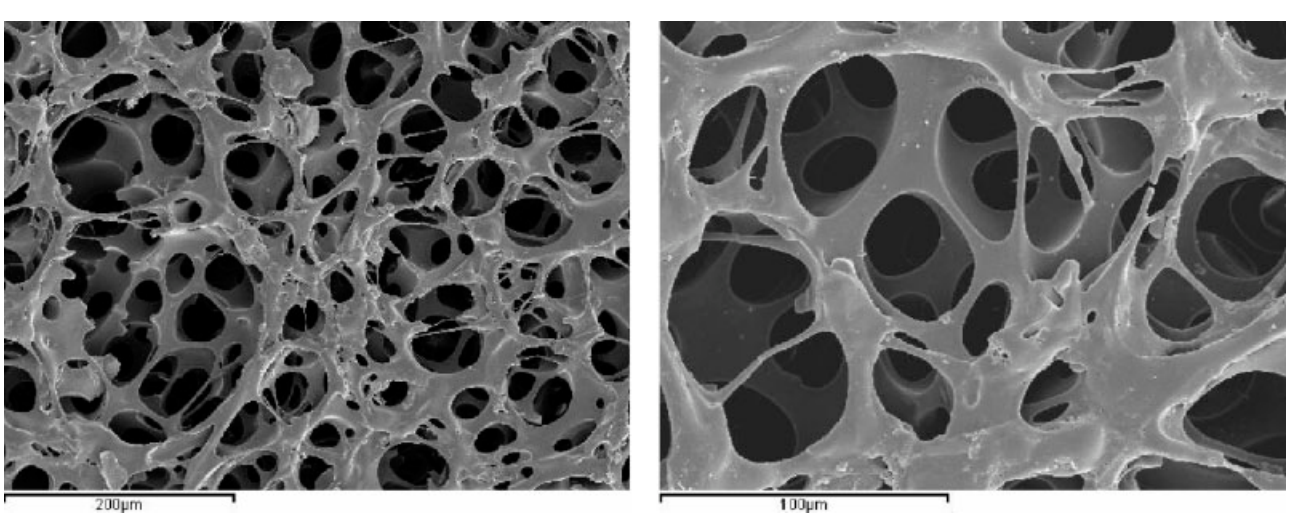

Figure 5 SEM micrographs of glassy polymer scaffolds. The matrix consists of a copolymer P(EMA-*co*-BA) crosslinked using EGDMA 1 wt %.

the glassy-like state prevents the pore collapse that would take place if the matrix were a rubber-like network, as previously (Fig. 5).

CONCLUSIONS

The pore collapse during the fabrication process of rubber-like polymer scaffolds was systematically studied. The enormous increase in the volume network as a consequence of the swelling process during the template extraction produces the shrinking of the porous structure when the system is dried. It has been shown that as the amount of crosslinking density in the scaffolding network increases (keeping the polymer–solvent interaction parameter) the open-interconnected structure is reached, preventing its collapse.

The pore collapse does not take place in glassy scaffolds even if the network swelling reaches high values and the polymer chains are equally highly stretched during the template extraction. The increase of T_g above room temperature as the network is dried explains this behavior.

References

1. Hutmacher, D. W. Biomaterials 2000, 21, 2529.
2. Hollister, S. J.; Maddox, R. D.; Taboas, J. M. Biomaterials 2003, 23, 4095.
3. Sun, W.; Darling, A.; Starly, B.; Nam J. J Biotechnol Appl Biochem 2004, 39, 29.
4. Langer R.; Vacanti, J. P. Science 1993, 260, 920.
5. Thomson, R. C.; Wake, M. C; Yaszemski, M. J.; Mikos, A. G. Adv Polym Sci 1995, 122, 245.
6. Langer, R. J Control Rel 1999, 62, 7.
7. Zhang, R.; Ma, P. X. J Biomed Mater Res 1999, 44, 446.
8. Thomson, R.; Shung, A. K.; Yaszemski, M.; Mikos, A. In Principles of Tissue Engineering; Lanza, R.; Langer, R.; Vacanti, J., Eds.; Academic Press: New York, 1997; Chapter 21.
9. Severian, D. Polymeric Biomaterials. Marcel Dekker: New York, 2002; 2nd Ed.
10. Karande, T. S.; Ong, J. L.; Agrawal, C. M. Ann Biomed Eng 2004, 32-12, 1728.
11. Gao, C. Y.; Wang, D. Y.; Shen, J. C. Polym Adv Technol 2003, 14, 373.
12. Whang, K.; Thomas, C. H.; Healy, K. E. Polymer 1995, 36, 837.
13. Harris, L. D.; Kim, B. S.; Mooney, D. J. J Biomed Mater Res 1998, 42, 396.
14. Thomson, R. C.; Wake, M. C.; Yaszemski, M. J.; Mikos, A. G.; Adv Polym Sci 1995, 122, 245.
15. Mikos, A. G.; Sarakinos, G.; Leite, S. M.; Vacanti, J. P.; Langer, R. Biomaterials 1993, 14, 323.
16. Zhou, Q.; Gong, Y.; Gao, C.; J Appl Polym Sci 2005, 98, 1373.
17. Brígido, R.; Pérez, M.; Serrano, A.; Gómez, J. L.; Monleón, M.; Gallego, G.; Salmerón, M. J Mater Sci-Mater M 2005, 16, 693.
18. Brígido, R.; Más, J.; Sanz, J. A.; García, J. M.; Salmerón, M. J Biomed Mater Res B, submitted.
19. Li, S.H.; De Wijn, J. R.; Layrolle, P.; De Groot, K. J Biomed Mater Res 2002, 61, 109.
20. Hedrick, J. L.; Russell, T. P.; Labadie, J.; Lucas, M.; Swanson, S. Polymer 1995, 36, 2685.
21. Lynch, I.; Dawson, K. A. Macromol Chem Phys 2003, 204, 443.
22. Perez, M.; Garcia-Giralt, N.; Monleón, M.; Benito, P.; Gómez, J. L.; Cáceres, E.; Monllau J. C. Biomaterials 2006, 27, 1003.
23. Bartolo de, L.; Morelli, S.; Bader A.; Drioli, E. Biomaterials 2002, 23, 2485.
24. Bruinsma, G. M.; Van Der Mei, H. C.; Busscher, H. J. Biomaterials 2001, 22, 3217.
25. Erbay, E.; Okay, O. J Appl Polym Sci 1999, 71, 1055.
26. Haeupke, H.; Pientka, V. J Chromatogr 1974, 102, 117.
27. Hilgen, H.; DeJong, G. J.; Sederel, W. L. J Appl Polym Sci 1975, 19, 2647.
28. Galina, H.; Kolarz, B. N. Polym Bull 1980, 2, 235.
29. Baldrian, J.; Kolarz, B. N.; Galina, H. Coll Czech Chem Commun 1981, 46, 1675.
30. Kolarz, B. N.; Wieczorek, P. P.; Wojczynska, M. Angew Makromol Chem 1981, 96, 193.
31. Wieczorek, P. P.; Ilavsky, M.; Kolarz, B. N.; Dusek, K. J Appl Polym Sci 1982, 27, 277.
32. Wieczorek, P. P.; Kolarz, B. N.; Galina, H. Angew Makromol Chem 1984, 126, 39.
33. Galina, H.; Kolarz, B. N.; Wieczorek, P. P.; Wojczynska, M. Br Polym J 1985, 17, 215.
34. Okay, O.; Balkas, T. I. J Appl Polym Sci 1986, 31, 1785.
35. Okay, O. J Appl Polym Sci 1986, 32, 5533.
36. Poinescu, I.; Vlad, C.; Carpov, A.; Ionid, A. Angew Makromol Chem 1988, 156, 105.
37. Cheng, C. M.; Vanderhoff, J. W.; El-Aasser, M. S. J Polym Sci Pol Chem Ed 1992, 30, 245.
38. Okay, O. Angew Makromol Chem 1986, 143, 209.
39. Okay, O. Angew Makromol Chem 1987, 153, 125.
40. Okay, O. Angew Makromol Chem 1988, 157, 15.
41. Takeda, K.; Akiyama, M.; Yamamizu, T. Angew Makromol Chem 1988, 157, 123.
42. Jun, Y.; Rongnan, X.; Juntan, Y. J Appl Polym Sci 1989, 38, 45.
43. Flory, P. J. Principles of Polymer Chemistry; Cornell Univesity Press: Ithaca, NY, 1953.